

Parity Asymmetry in the CMBR Temperature Power Spectrum

Pavan K. Aluri^{*}, Pankaj Jain[†]

Department of Physics, Indian Institute of Technology, Kanpur 208016, India

Abstract: We study the power asymmetry between even and odd multipoles in the multipolar expansion of CMB temperature data from WMAP, recently reported in the literature. We introduce an alternate statistic which probes this effect more sensitively. We find that the data is highly anomalous and consistently outside 2σ significance level in the whole multipole range $l = [2, 101]$. We examine the possibility that this asymmetry may be caused by the foreground cleaning procedure or by residual foregrounds. By direct simulations we rule out this possibility. We also examine several possible sub-dominant foregrounds, which might lead to such an asymmetry. However in all cases we are unable to explain the signal seen in data. We next examine cleaned maps, using procedures other than the one followed by the WMAP Science team. Specifically we analysed the maps cleaned by the IPSE procedure, Needlets and the harmonic ILC procedure. In all these cases we also find a statistically significant signal of power asymmetry if the power spectrum is estimated from masked sky. However the significance level is found to be not as high as that in the case of WMAP best fit power spectrum. Finally, we test for the contribution of low- l multipoles to the observed power asymmetry. We find that if we eliminate the first six multipoles, $l = [2, 7]$, the significance falls below 2σ CL. Hence we find that the signal gets dominant contribution from low- l modes.

1 Introduction

The primary aim of WMAP satellite has been to measure full sky CMBR temperature anisotropies with great precision (Bennett et al., 2003a). The primary quantity of interest from these full sky maps is the temperature power spectrum, which is used to constrain various cosmological parameters (Hinshaw et al., 2003; Spergel et al., 2003; Larson et al., 2011; Komatsu et al., 2011). It also gave TE cross power spectrum and E-mode power to a good precision (Kogut et al., 2003; Page et al., 2003; Larson et al., 2011; Komatsu et al., 2011). Since the release of WMAP 1st year data many large scale anomalies were reported in the data (Bennett et al., 2003b, Efstathiou, 2003; de Oliveira-Costa et al., 2004; Eriksen et al., 2004a,b; Ralston & Jain, 2004; Copi & Huterer, 2004; Schwarz et al., 2004; Land & Magueijo, 2005a; de Oliveira-Costa & Tegmark, 2006; Copi et al., 2007; Samal et al., 2008; Copi et al., 2010; Bennett et al., 2011). Recently, in (Kim & Naselsky, 2010), (see also de Oliveira-Costa et al., 2004; Land & Magueijo, 2005b; Gurzadyan et al., 2007; Gruppuso et al., 2011; Hansen et al., 2011; Ben-David, Kovetz & Itzhaki, 2011), it was found that the CMB power in odd multipoles is anomalously more than that in the even multipoles. Some possible sources of such odd modulations to CMB, like signals from inflationary era and solar system physics, were discussed in (Groeneboom et al., 2010; Koivisto & Mota, 2011; Maris et al., 2011). This power asymmetry between even and odd multipoles is also addressed as *Parity asymmetry*.

The CMBR temperature fluctuations on a sphere are usually expanded in terms of spherical harmonics, Y_{lm} , as

$$\Delta T(\theta, \phi) = \sum_{l=0}^{\infty} \sum_{m=-l}^{+l} a_{lm} Y_{lm}(\theta, \phi), \quad (1)$$

^{*}email: aluri@iitk.ac.in

[†]email: pkjain@iitk.ac.in

where a_{lm} 's are the multipolar expansion co-efficients. The power spectrum of CMB is defined as

$$C_l = \frac{1}{2l+1} \sum_{m=-l}^{+l} a_{lm}^* a_{lm}. \quad (2)$$

We denote $\mathbb{C}_l = l(l+1)C_l/2\pi$. Kim & Naselsky (2010) defined the following two quantities

$$P^+ = \sum_{l=2}^{l_{max}} \frac{(1+(-1)^l)}{2} \mathbb{C}_l \quad (3)$$

and

$$P^- = \sum_{l=2}^{l_{max}} \frac{(1-(-1)^l)}{2} \mathbb{C}_l. \quad (4)$$

Here P^+ and P^- represent the sum of power in the even and odd multipoles respectively. The parity asymmetry statistic was defined as P^+/P^- , which we refer to as “ $P(l_{max})$ ” for convenience. By comparing the data (Larson et al., 2011) with “pure” realizations of CMB signal generated based on Λ CDM model, they estimated the p -value to be 0.002. When this statistic was applied on full-sky C_l recovered from masked maps, using $KQ85$ mask from WMAP’s seven year data release, the minimum probability or p -value was found to be $p = 0.003$. The l_{max} corresponding to this p -values was found to be 22 from simulations, which is an *a posteriori* choice. By accounting for this posterior choice of $l_{max} = 22$, the probability was estimated to have lowered to 0.02.

In the present paper we study this parity asymmetry in considerable detail. We first consider an alternate statistic to test for parity asymmetry. This statistic is found to be more sensitive than the one considered in (Kim & Naselsky, 2010). We next investigate whether this asymmetry might arise due to foregrounds, which are not symmetric under parity. Most of the foreground contamination, however, gets removed in the process of extracting the primordial power spectrum. Nevertheless the residual foregrounds might be sufficiently large to cause parity asymmetry. Hence we use simulated foreground cleaned maps to test the significance of parity asymmetry in the WMAP CMBR data. We utilize both the ILC and IPSE cleaning procedure for this purpose. The simulated maps are generated using random realizations of CMBR and pre-launch Planck Sky Model for foregrounds. We also allow for the possibility of some unknown foreground components. Another interesting anomaly found in the CMB data is the ecliptic dipolar modulation of the CMB power, discovered in (Eriksen et al., 2004a). This signal is also parity asymmetric and hence one may suspect that there might be a relationship between this and the signal discovered in (Kim & Naselsky, 2010). We study the possibility that a dipole modulation of temperature anisotropy might lead to the observed parity asymmetry. Furthermore we examine whether foreground cleaned maps obtained using alternate procedures such as IPSE, Needlet ILC, etc., also show the parity asymmetry observed in the WMAP best fit power spectrum. Finally we determine the contribution of the modes at very low l to the observed asymmetry.

This paper is arranged as follows. In the next section, a different statistic to understand this even-odd power asymmetry is presented. Then, in section 3 we present our results obtained from mock cleaned data used to test the effect of foreground residuals. In section 4 we explore the effect of unknown influences on the data which might be modulating the primordial signal to induce the observed power asymmetry. In section 5 we present our analysis of parity asymmetry in IPSE cleaned temperature data and the cleaned maps available using other procedures such as Needlet ILC, etc. In section 6, our results from implementing different cut at various low- l modes are shown. Finally, we conclude in section 7.

2 An Alternate Statistic

In this section we introduce a different statistic to quantify the parity asymmetry. As we shall see this statistic is a more sensitive probe than the one given in Eqs. [3] and [4]. Instead of taking averages of ' l ' even or odd multipoles, we look at local ' l ' power asymmetry. It is defined as¹

$$Q(l_{odd}) = \frac{2}{l_{odd} - 1} \sum_{l=3}^{l_{odd}} \frac{C_{l-1}}{C_l}, \quad (5)$$

where the maximum, l_{odd} , is any odd multipole $l \geq 3$ and the summation is over all odd multipoles upto l_{odd} . Thus $Q(l_{odd})$ is a measure of mean deviation of the ratio of power in an even multipole to its succeeding odd multipole from one, if it is present in the data. At low- l , since $l(l+1)C_l \sim \text{constant}$, statistically we expect our statistic to fluctuate about one, like $P(l_{max})$.

3 Statistical Significance of parity asymmetry using pure and foreground cleaned CMBR maps

We test the WMAP seven year best fit CMB temperature power spectrum² for anomalous parity asymmetry against both pure realizations of CMBR and simulated cleaned maps. The pure CMB sky maps are generated as constrained realizations of best fit theoretical CMB power spectrum from Λ CDM model². The **synfast** facility of freely available **HEALPix**³ software (Gorski et al., 2005) was used to produce full sky pure CMB realizations at $N_{side} = 512$ of **HEALPix**'s sky pixelization scheme. We then generate five raw maps corresponding to each frequency channel in which WMAP makes the observations. We do so by adding the pure CMB maps with synchrotron, thermal dust and free-free emission templates from the pre-launch Planck Sky Model (PSM)⁴ (PLANCK Blue Book, 2005) available in each of the WMAP's frequency bands. These maps were convolved with appropriate beam transfer functions of K, Ka, Q, V and W bands of WMAP² simulating the raw satellite data. We have also added Gaussian random noise in each pixel using the mean rms noise levels in each of the WMAP's frequency channels provided in its seven year data release (Jarosik et al., 2011). Strong foreground contamination to the observed cosmic CMB signal are assumed to be due to galactic synchrotron, dust and free-free emissions. Synchrotron radiation is emitted from relativistic electrons in cosmic rays spiraling into the galactic magnetic field. When the dust grains in the interstellar medium get heated, they emit radiation due to vibrational mode transitions in infrared frequency which is the thermal dust emission. The free-free emission is due to the electron-ion interactions in the ionized medium between clusters of galaxies. The full sky simulated raw maps thus generated were cleaned using IPSE method as described below.

3.1 IPSE cleaning procedure

Here we briefly outline the cleaning procedure we employ to clean the simulated raw maps. The IPSE cleaning procedure (Tegmark, de Oliveira-Costa & Hamilton, 2003; Saha, Jain & Souradeep, 2006; Eriksen et al., 2007a; Saha et al., 2008; Samal et al., 2010) is a minimum variance optimization method better suited for multi-channel CMB observations such as WMAP and PLANCK. It exploits the frequency dependence of astrophysical foregrounds received in various detection channels, enabling us to efficiently extract the

¹While compiling the references to our present work, we learnt that a similar, but not identical, statistic was used by (Land and Magueijo, 2005b), which was referenced in the introduction.

²Available at <http://lambda.gsfc.nasa.gov/>

³Available at <http://healpix.jpl.nasa.gov/>

⁴<http://www.planck.fr/healing79.html>

cosmic signal. The method involves linearly combining various multi-channel maps in multipole space with appropriate weights as

$$a_{lm}^{clean} = \sum_{i=1}^{n_c} \hat{w}_l^i \frac{a_{lm}^i}{B_l^i}, \quad (6)$$

where a_{lm}^{clean} is the clean CMB signal extracted from the raw data, a_{lm}^i , acquired from measurements in n_c frequency channels by linearly combining them with appropriate weights \hat{w}_l^i . The B_l^i factors are the symmetrized beam transfer functions in multipole space corresponding to an i^{th} frequency channel. The weights are computed using the empirical covariance matrix,

$$\hat{C}_l^{ij} = \frac{1}{2l+1} \sum_{m=-l}^{+l} a_{lm}^{i*} a_{lm}^j, \quad (7)$$

in the formula,

$$\hat{\mathbf{W}}_l = \frac{\mathbf{e}_0^T \hat{\mathbf{C}}_l^{-1}}{\mathbf{e}_0^T \hat{\mathbf{C}}_l^{-1} \mathbf{e}_0}, \quad (8)$$

where $\mathbf{e}_0 = (1...1)^T$ is a column vector with n_c unit elements and $\hat{\mathbf{W}}_l$ is also a column vector given by $(\hat{w}_l^1 \dots \hat{w}_l^{n_c})^T$. The clean power spectrum is then given by,

$$\hat{C}_l^{clean} = \frac{1}{\mathbf{e}_0^T \hat{\mathbf{C}}_l^{-1} \mathbf{e}_0}. \quad (9)$$

Further, taking into account the spatial variation of the foreground power across the sky, each map is divided into disjoint sky regions and this procedure is applied iteratively in each of these sky partitions.

Using the IPSE cleaning procedure we generated an ensemble of 800 cleaned maps. A residual foreground bias correction was implemented on each of the cleaned maps by subtracting a bias map estimated from these simulations in pixel space (Bennett et al., 2003c). The power spectrum of each of these simulated maps was computed using the **anafast** facility of **HEALPix** and corrected for beam and pixel window effects. We used full sky cleaned maps' power spectrum for the range $l = [2, 10]$. The low- l power can be recovered reliably from full sky cleaned maps using the IPSE method (Tegmark, de Oliveira-Costa & Hamilton, 2003). For $l \geq 11$, we used full sky C_l recovered from partial sky map we get after applying a galactic mask excluding the heavily contaminated regions in the sky. The *KQ85* mask² provided by WMAP science team in their seven year data release was applied on the simulated maps and we recovered the full-sky C_l using the MASTER of CMBR or pseudo- C_l estimator (Hivon et al., 2002). At low- l , up to $l = 32$, the WMAP best fit power spectrum is estimated from a low resolution ILC map by using the Blackwell-Rao likelihood estimator (Larson et al., 2011). For $l > 32$, they estimated the multipole power using the same pseudo- C_l estimator that we use to estimate C_l at high- l . These power spectra form the basis of our analysis.

3.2 Statistical significance

We next compute the statistical significance using both the statistics, $P(l_{max})$ and $Q(l_{odd})$, given in Eqs. [3, 4] and Eq. [5] respectively. We used the best fit CMB temperature power spectrum from WMAP's seven year data release as reference data. The values of both the statistics for the best fit power are shown in Fig. [1].

The random chance occurrence probability of getting a $P(l_{max})$ lower than that of the data for $l_{max} \in [3, 101]$ is shown in Fig. [2]. For the case of pure maps we used an ensemble of 10,000 simulated CMBR maps. We reproduce the results from (Kim & Naselsky, 2010) using the pure maps ensemble with lowest probability at $l_{max} = 22$. From the 10,000 pure maps we generated, the probability was found to be 0.0013.

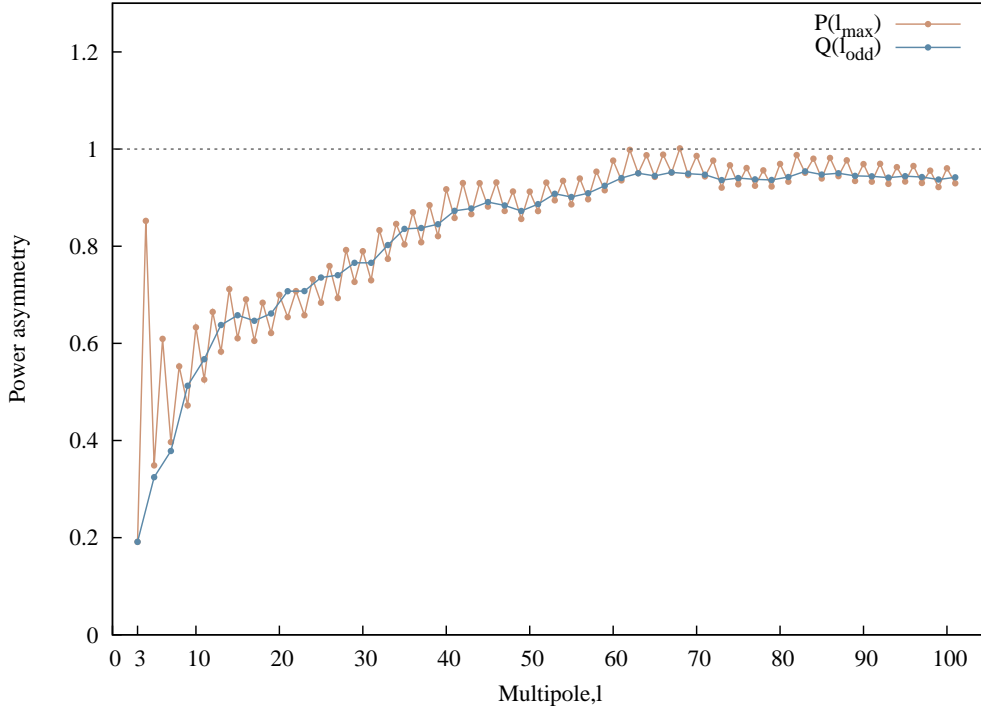


Figure 1: The even-odd multipole power asymmetry in WMAP’s seven year best fit temperature power spectrum in the multipole range $l = [2, 101]$ is shown. The asymmetry is computed using both the $P(l_{max})$ statistic (lighter curve) and our parity asymmetry statistic, $Q(l_{odd})$ (darker curve).

Also, presented in the graph are significances computed using the cleaned maps ensemble. In this case we used only 800 simulated maps due to constraints on computational time. As can be seen, the p -values from cleaned maps are slightly higher than the probability estimates from pure maps, but are relatively close. The foreground power have strong even parity preference and, in (Kim & Naselsky, 2010), the authors speculated that the observed asymmetry could be due to over subtraction of foregrounds during foreground reduction. But, eventually they ruled out this possibility. Using cleaned maps, we confirm that this is indeed the case. Thus, any residual foreground contamination present in the cleaned maps may not induce a particular parity preference in the data. The contribution of noise is negligible to the power at low- l . Since, we studied this power asymmetry in a wider multipole range, up to $l = 101$, and incorporated noise in the simulated raw maps, we also conclude that noise cannot cause this asymmetry. From the ensemble of cleaned maps, the lowest probability for this parity asymmetry is again found to be at $l_{max} = 22$ with a chance probability of 0.13%. This minimum value for significance is beyond 3σ CL and quickly falls below 2σ CL by around $l_{max} = 40$. Beyond $l_{max} = 40$ it largely stays below 2σ . One interesting thing to note is that the $P(l_{max})$ curve in Fig. [1] looks wavy, like it was overlayed by some oscillations. It may be indicative of the presence of some underlying modulation (see for example Turner, 1983; Martin & Ringeval 2004, 2006; Wang et al., 2005; Ichiki, Nagata & Yokoyama, 2010).

With our estimator $Q(l_{odd})$, we find that, in almost the entire multipole range $l = [2, 101]$, the significance of the parity asymmetry lies consistently outside 2σ CL in both cases using the pure maps and the cleaned maps. These probability estimates are shown in Fig. [3]. The only exceptions are the significances of the multipoles 63, 67 and 69 with the cleaned maps ensemble which are marginally inside the 95% CL. Since, $P(l_{max})$ involves the sum of all even or odd multipole power up to a chosen l_{max} , which is equivalent to the mean power up to that l_{max} , it appears that their sum is hiding the true significance. As can be seen from the plot, we find that for $l \in [18, 31]$ the significance of parity asymmetry using $Q(l)$ on WMAP’s seven

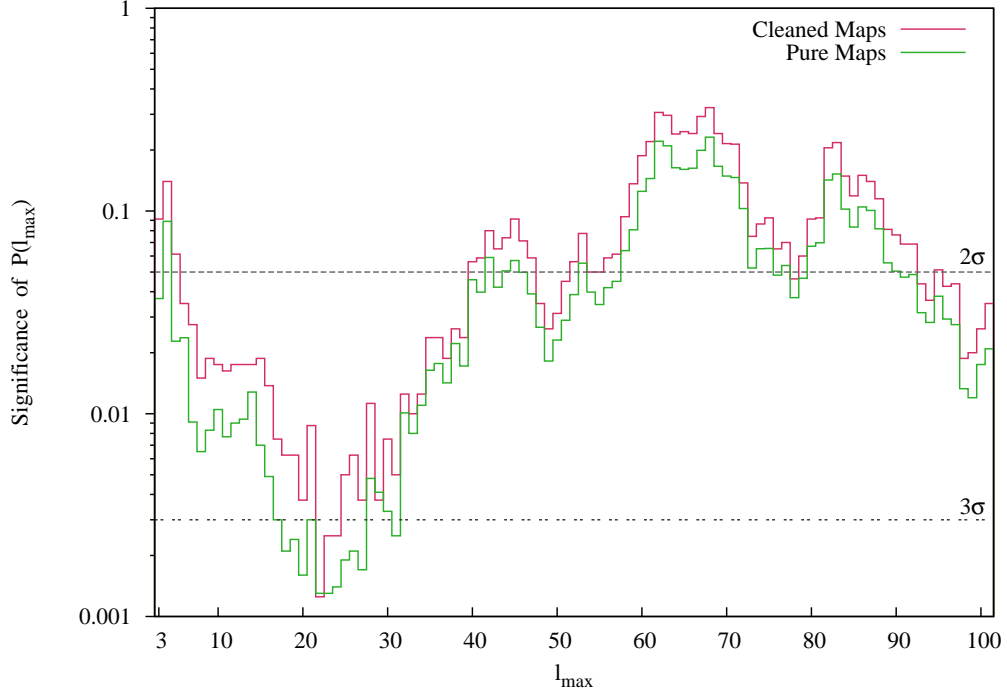


Figure 2: Probability estimates of parity asymmetry seen in the data using the $P(l_{max})$ parity statistic, in the multipole range $l = [2, 101]$. The significances are computed using 10,000 pure maps and 800 cleaned maps, cleaned using IPSE method. We find no significant difference between the two estimates. As can be seen, the most significant results occurs at $l = 22$ for both the cases and is beyond 3σ CL.

year best fit temperature C_l is outside 3σ as estimated from pure maps with minimum at $l = 19$. In (Kim & Naselsky, 2010), $l_{max} = 22$ is specially singled out, for the p -value is lowest at that l_{max} . Here, we see that the p -values of $Q(l)$ in the range $l = [18, 31]$ remain close to their minimum. Hence we don't attribute any special significance to a particular multipole where $Q(l)$ is minimum, but rather to the whole range $l = [18, 31]$. With the cleaned maps simulated set, we find that the p -value curve has slightly risen, but only slightly in comparison to that of pure maps. Hence we argue that residuals in the cleaned data cannot cause the observed power asymmetry between even and odd multipoles. In the case of cleaned maps, the minimum probability for this parity asymmetry is found in the range $l = [22, 33]$ using our statistic.

In our analysis above we used the IPSE cleaning procedure on the simulated maps. It is clearly better to use the same procedure for cleaning both the observed data as well as the simulated maps. We do this in section 5.1 where we use the ILC cleaning procedure uniformly for the entire analysis. As we shall see the results in that case are also consistent with those obtained in the present section.

4 Unknown foregrounds

The even-odd multipole power asymmetry we are studying is a point inversion (PI) symmetry violation. So, we constructed some templates with explicit PI symmetry breakdown which may induce a power excess in odd multipoles and incorporate them in generating our simulated raw maps. In (Dobler & Finkbeiner 2008a), an anomalous haze component was found in the WMAP data. It could be that this anomalous haze has such asymmetry. Also, there are sub-dominant foregrounds in microwave frequency region which are not well characterized yet (Kogut et al., 1996; de Oliveira-Costa et al., 2002; Dobler & Finkbeiner 2008b). However, instead of making any such identifications here, we pursue the analysis including these new templates as

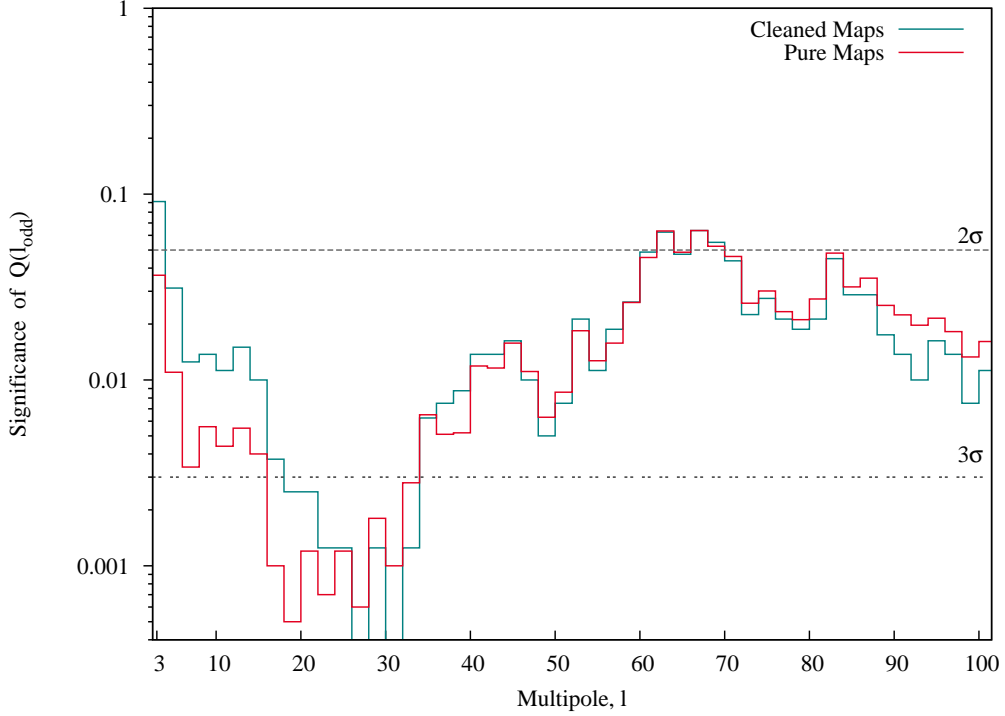


Figure 3: The p -values of $Q(l_{\text{odd}})$ for WMAP 7 year best fit power spectrum are shown here. As can be seen, the data is consistently anomalous by being outside 2σ in the whole multipole range $l = [2, 101]$. For the case of cleaned maps, a value less than $1/800$ indicates that we obtained no simulated maps whose statistic was smaller than that of observed data.

some hitherto unknown components. A readily conceivable pattern with such a point symmetry violation is a hemispherical power asymmetry. This template is shown in Fig. [4] at the top. We scale this template by a small factor before including them in simulated raw data production pipeline so that it's contribution stays sub-dominant and that the simulated raw maps conform visually with the accumulated raw data from observations. The results presented in this section were obtained using 350 simulations. Since, we were expecting to find a lower significance of parity asymmetry in the presence of asymmetric foregrounds, 350 simulations are sufficient to probe it up to 3σ CL.

We used this template in two ways, one in which this template is scaled from K-band to W-band of WMAP by a frequency dependent power law function and in the other instance as a constant asymmetric foreground component, constant in all frequency channels. In the former case, we chose the scaling factor to be $1/15^{\text{th}}$ the monopole intensity of synchrotron from PSM at 23GHz ($99\mu K$). It is further scaled to W-band following rigid frequency scaling (Bouchet & Gispert, 1999) with a steep spectral index as $F(\nu) = F(\nu_0)(\nu_0/\nu)^{2.8}$, where $F(\nu_0)$ is the intensity distribution of a foreground component at a reference frequency ν_0 extrapolated to another frequency ν . We chose a large spectral index so that this effect dies off at higher frequencies (V or W bands) where CMB is supposed to be less contaminated by the foregrounds. These templates, generated at five frequency bands of WMAP, were added to raw maps and convolved with appropriate beam function. In the latter case, where this asymmetric map is added as a fixed power in each pixel across all bands, it is scaled by $1/30^{\text{th}}$ the synchrotron monopole intensity at 23GHz. The scaling factor is chosen such that this excess power will stay lower than the three dominant foregrounds in each channel. The results are presented in Fig. [5] using our statistic.

We find that the significance decreases, but only a little in both the cases. These probability estimates are similar to either pure maps or cleaned maps with only the three dominant foreground components from

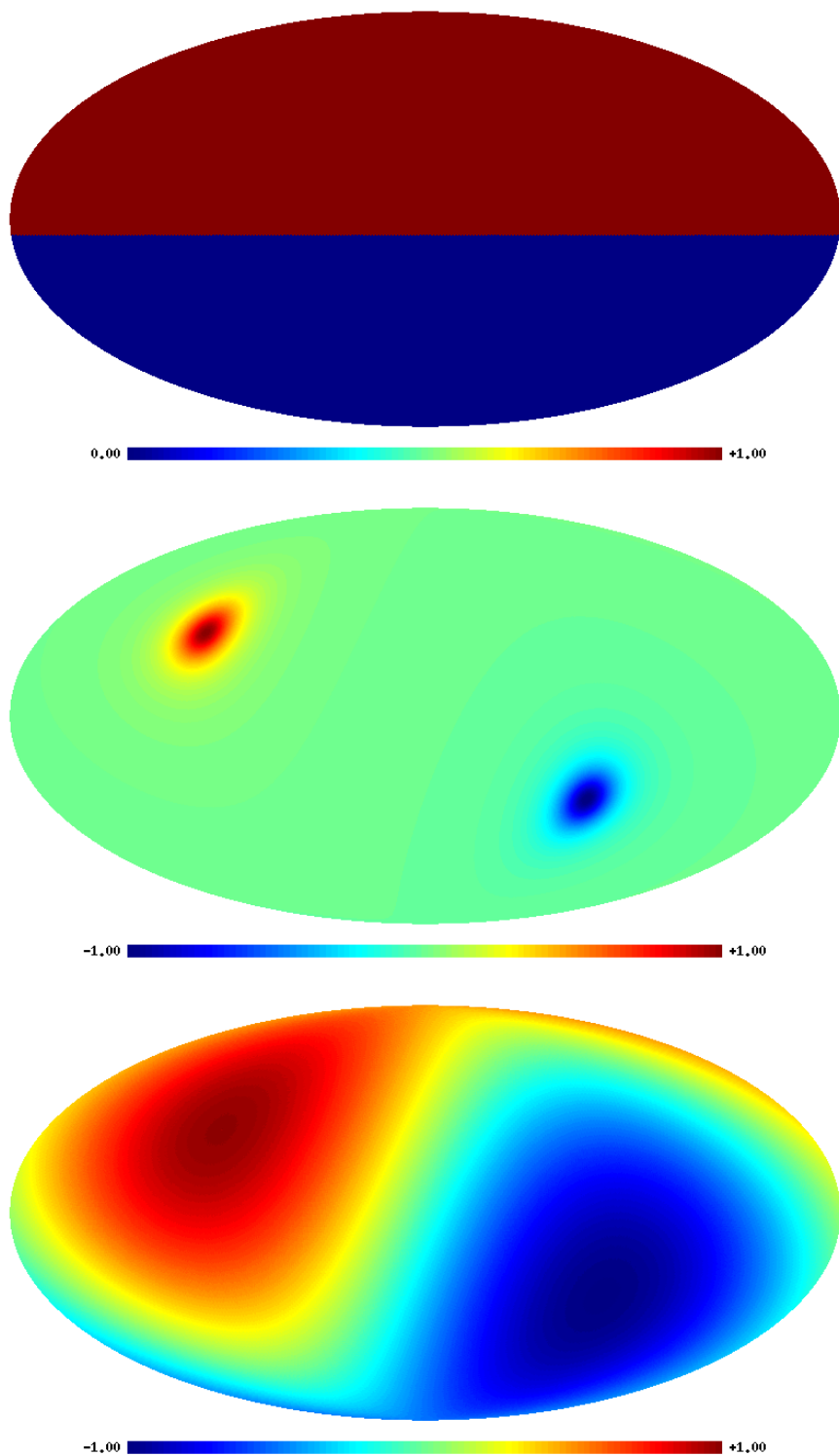


Figure 4: Various explicitly power asymmetric templates used in our analysis. These are generated by modifying some of the `HEALPix` routines. The middle and the bottom ones are used in our studies to relate North-South ecliptic power asymmetry found by Eriksen *et al.* (2004a) and the parity asymmetry that we are studying here.

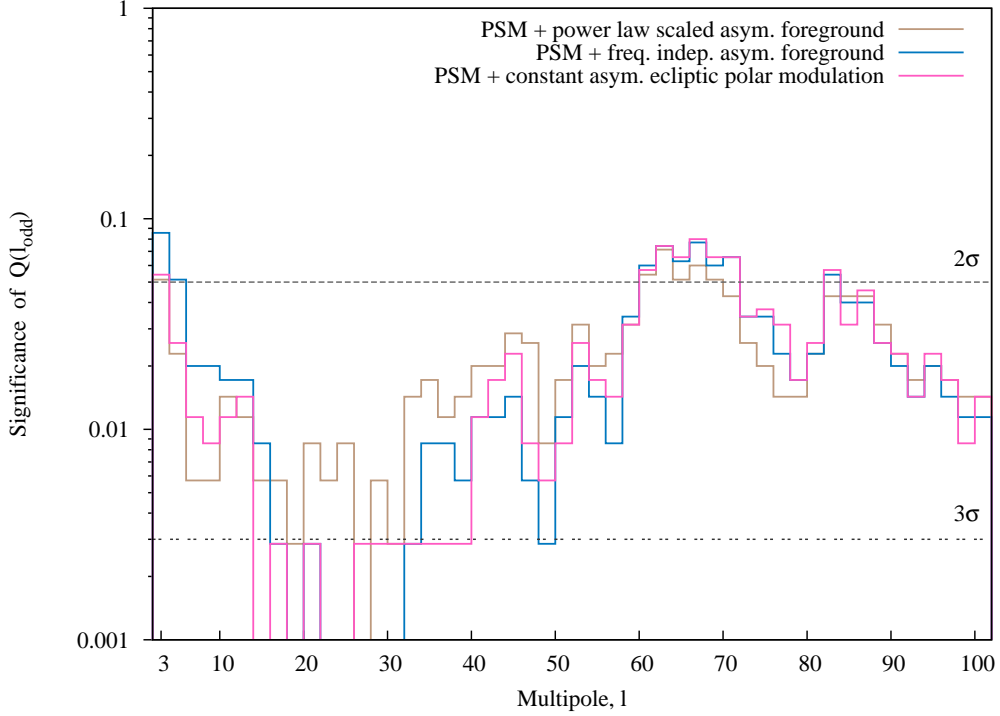


Figure 5: The p -value plot from the simulated ensemble set generated including our hitherto unknown foreground maps with explicit point inversion asymmetry using the $Q(l_{odd})$ statistic. The significances given here are for (1) power law scaled PI asymmetric map, (2) a constant power asymmetric map and (3) a foreground component which has explicit power asymmetry in its even and odd multipoles.

PSM. We also used exponentially scaled prefactors for this template and found no increase in probability, as a test for foreground components which may not be following polynomial scaling laws.

Then, we generated another template which is explicitly asymmetric in power between even and odd multipoles. We generated a_{lm} 's with non-zero values for only a_{l0} 's and zero otherwise and that the asymmetry dies (exponentially) with increasing l . The generated map is also shown in Fig. [4], in the middle. Eriksen *et al.* (2004a) found a hemispherical power asymmetry between the north and south ecliptic hemispheres. Motivated by the similarity of the that North-South power asymmetry and PI symmetry violation, we explore whether there is any relation between these two phenomena. So, we rotate this explicitly even-odd power asymmetric map into ecliptic poles. This template is scaled by $1/20^{th}$ the monopole intensity of synchrotron map from PSM and added it as a constant ecliptic dipolar power excess. Here we used a slightly higher power to scale this template compared to the earlier constant hemispherical asymmetric template.

Again we find no change in significance. It only decreases marginally. To find any significant effect with this template, we had to add it at unrealistically high levels. With low intensity level, we do not find any increase in probability. The significance estimates with our statistic, $Q(l)$, for this dipolar modulation are also shown in Fig. [5]. In Fig. [6], we presented the p -value estimates using the $P(l_{max})$ statistic.

4.1 Multiplicative modulation

So far we explored the possibility of only “additive” modulations to the data. Now, we also consider “multiplicative” modulations (Gordon et al., 2005; Eriksen et al., 2007b; Bunn & Bourdon, 2008; Hanson & Lewis, 2009) which can break PI symmetry. The proposed modulation to the CMB is

$$\Delta T(\hat{n}) = \Theta(\hat{n})(1 + A\hat{\lambda} \cdot \hat{n}), \quad (10)$$

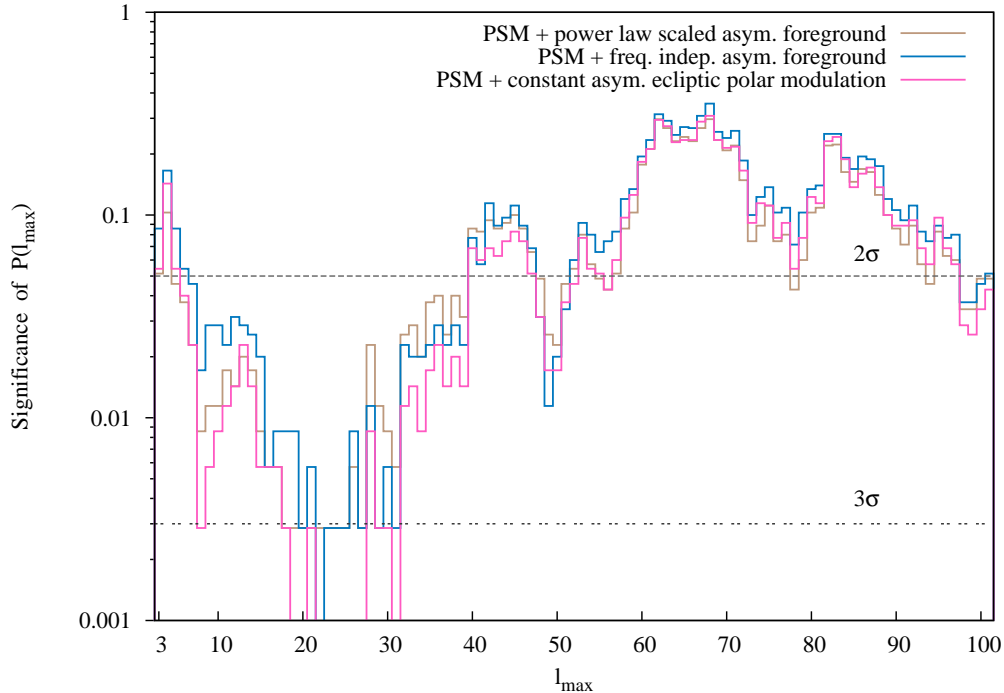


Figure 6: Same as Fig. [5], but for the $P(l_{max})$ statistic

where A is the modulation amplitude and $\hat{\lambda}$ is the preferred direction. We chose $\hat{\lambda}$ to lie along the axis of ecliptic poles. Thus, we generated a dipole modulation map of Eq. [10] also shown in Fig. [4], at the bottom.

Even with an amplitude of $A = 0.3$ we find that it cannot induce a particular parity preference. The results from modulated pure maps are shown in Fig. [7]. Also shown there are the pure maps estimates for comparison. When the same modulation is applied on the raw maps, there is an enhancement in the parity asymmetry in the cleaned map, Fig. [7]. This enhancement of power asymmetry in modulated raw maps suggest a measurement artifact rather than any thing fundamental to CMB radiation. We point out that we are using $A = 0.3$ which is relatively large amplitude for modulation. Even with such a large amplitude, we don't find much change in the statistic's values of modulated pure maps compared to pure maps themselves.

5 IPSE and others

We next test the signal of parity asymmetry in maps cleaned by IPSE and several other procedures. In the case of IPSE we perform a full sky cleaning of the temperature raw data from WMAP's seven year data release. The power spectrum is computed from full sky cleaned map up to $l = 10$ and used pseudo- C_l estimator at higher l after applying WMAP's *KQ85yr7* mask. Later we estimate the power at low- l also from masked sky. This allows us to determine the how the parity statistic is influenced by masking. The $Q(l)$ and $P(l_{max})$ values in the range $l = [2, 101]$ for this power spectrum are shown in Fig. [8] and the probability estimates are shown in Fig. [9]. These p -values are computed from 10,000 simulated pure maps.

We see that the IPSE cleaned data does not show significant power asymmetry. It was surprising to find this result, given that the WMAP seven year best fit power spectrum is found to be highly anomalous. So, we also applied the two statistics to other cleaned maps available to us. The maps considered here are (1) cleaned map from WMAP's five year raw data⁶ obtained by using the procedure given in Tegmark, de

⁶<http://space.mit.edu/home/tegmark/wmap/> or <https://www.cfa.harvard.edu/~adeolive/gsm/index.html>

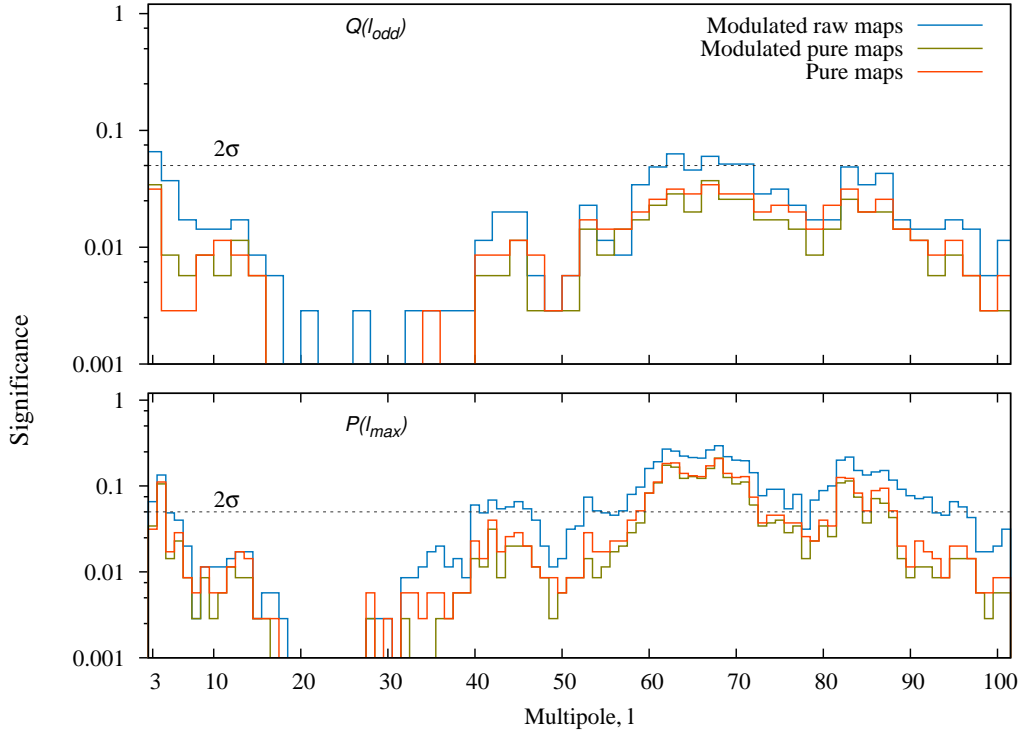


Figure 7: The p -values obtained after applying a dipolar multiplicative modulation to pure maps and raw maps before cleaning is shown here. The parity statistics of modulated pure maps are not different from the pure maps themselves. But the modulated raw maps show a slight decrease in the significance of power asymmetry.

Oliveira-Costa & Hamilton, 2003, (2) Needlet ILC map⁷ of (Delabrouille *et al.*, 2009) using WMAP’s five year data and (3) Harmonic ILC⁸ of (Kim, Naselsky & Christensen, 2008), which is also produced from WMAP five year data. We note that the maps (1) and (2) are available at resolution of W-band, just like IPSE cleaned map. But the Harmonic ILC map is available at 1° resolution. In all these cases the power is obtained from the full sky cleaned map up to $l = 10$ and pseudo- C_l estimator for $l > 10$, as in the case of IPSE. The parity asymmetry statistic values of these maps are also shown in Fig. [8]. As can be seen, all these maps give results close to each other, but do not agree with those obtained using the WMAP seven year best fit temperature power spectrum. Hence their significances are similar to IPSE cleaned data, as shown in Fig. [9].

The power spectrum in all the cases analysed in this section is obtained from full sky up to $l = 10$ and masked sky for $l > 10$. This is in contrast to the WMAP best fit power spectrum which uses masked sky over the entire multipole range. Hence it is useful to determine how the results for the maps considered in this section change if we use a pseudo- C_l estimator for $l \leq 10$ also. In order to estimate parity asymmetry using masked sky over the entire multipole range, we applied the WMAP’s *KQ85yr7* mask on all these cleaned maps including our IPSE map. We then obtained the corresponding full sky pseudo- C_l values for these maps. The corresponding significance of the parity asymmetry, using both the statistics, is shown in Fig. [10]. With our statistic, we find that all the different maps are relatively close to the WMAP’s best fit power spectrum. The $P(l_{max})$ statistic also shows a higher significance in comparison to the full sky power spectra. Hence, we find that, pseudo- C_l estimator, recovered from masked clean maps, reveals the presence of anomalous parity asymmetry in these maps. This is most likely due to the fact that the full sky has many heavily contaminated regions where the cleaning may not be very efficient. By masking such regions

⁷http://www.apc.univ-paris7.fr/APC_CS/Recherche/Adamis/cmb_wmap-en.php

⁸<http://www.nbi.dk/~jkim/hilc/>

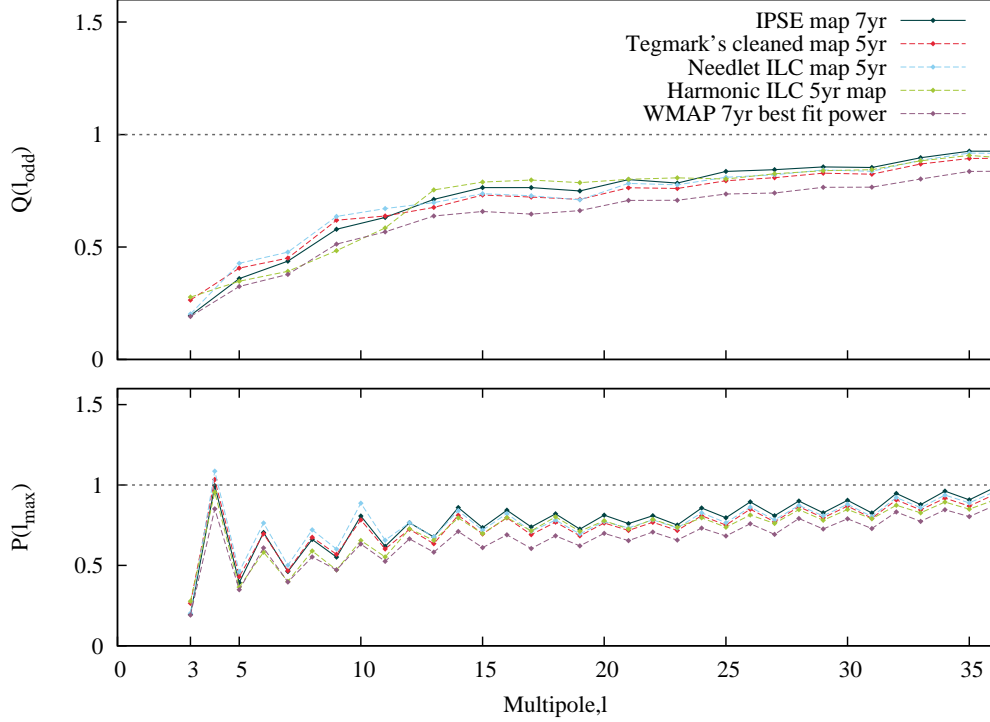


Figure 8: The parity statistic values using $Q(l)$ (top panel) and $P(l)$ (bottom panel) applied to cleaned maps, using several different procedures, are shown here. The maps used are (1) IPSE map, (2) Tegmark’s five year cleaned map, obtained using the procedure described in Tegmark, de Oliveira-Costa & Hamilton, 2003, (3) Needlet ILC five year map and (4) Harmonic ILC five year map. Also plotted are the power asymmetry statistic values for WMAP’s seven year best fit temperature power spectrum for comparison. All these maps show similar levels of parity asymmetry, but do not agree with WMAP’s best fit data.

we hope to get a better estimate of the true power spectrum of the CMB signal. It has been found earlier that some of the large angle anomalies disappear in cut sky maps (Bielewicz et al., 2005; Bernui et al., 2007; Efstathiou, Ma & Hanson, 2010; Pontzen & Peiris, 2010; Copi et al., 2011). It is therefore encouraging that in the present case the signal is enhanced rather than diminished when we use masked sky.

The fact that a pseudo- C_l estimator gives a higher significance of parity asymmetry in comparison to the power spectrum obtained from full sky may lead one to suspect that the process of masking itself might generate some signal of parity asymmetry. In order to study this possibility we determine the significance of parity asymmetry in WMAP best fit power spectrum by using simulated masked random realizations of pure CMB. We use the *KQ85yr7* for this purpose. The resulting significance levels for both the statistics are shown in Fig. [11]. For comparison we also show the results for the case when the power spectrum of the simulated maps are obtained from full sky. We find that if we use the masked sky pseudo- C_l estimator for the random samples, the significance level for parity asymmetry is slightly lower for both the statistics. Though there is a net rise in p -values due to masking, the relative change is marginal/low and the signal of anomalous parity asymmetry is still present.

5.1 Statistical significance using the ILC procedure for foreground removal

So far we have used the WMAP best fit power spectrum in our analysis. We computed the statistical significance by comparing the statistic for the best fit power with that obtained from the randomly generated pure CMB maps as well as simulated, foreground cleaned CMB maps. The simulated CMBR maps were cleaned using the IPSE procedure. We have also studied the parity asymmetry in other cleaned maps obtained

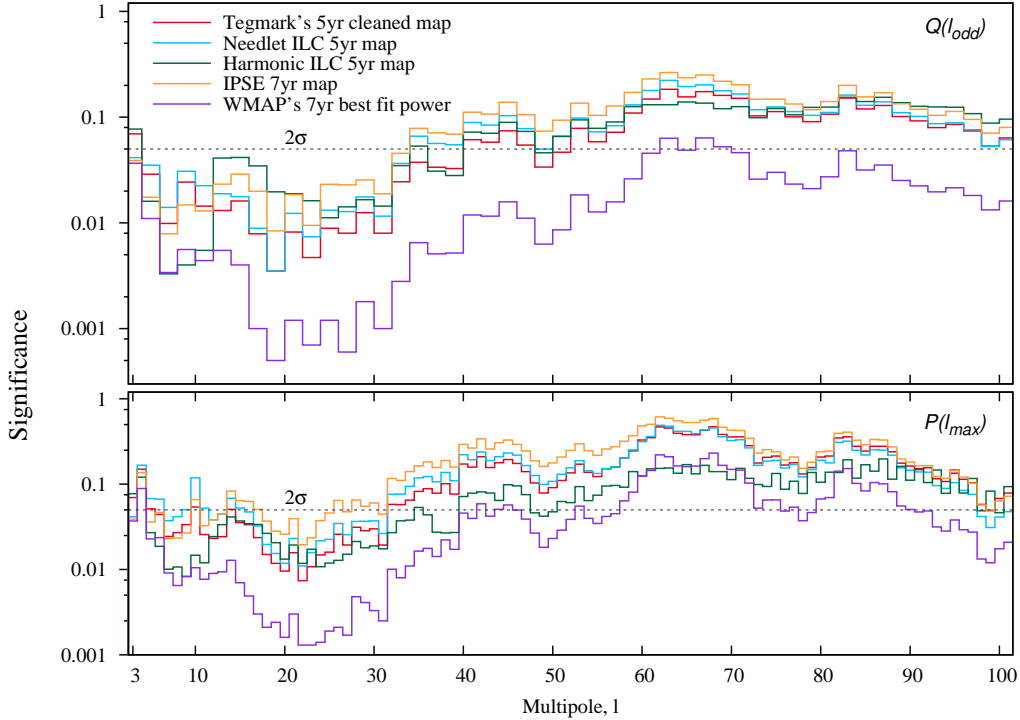


Figure 9: The p -values for parity asymmetry for the cleaned maps using several different procedures (see text).

using various procedures. In this section we compute the statistical significance using the ILC procedure for foreground removal. The ILC procedure is used both for estimating the statistic for the WMAP data as well as for cleaning the simulated maps.

In the ILC procedure, foregrounds are removed by making linear combination of maps at different frequencies in pixel space. Maps at different frequencies are smoothed to a common resolution of 1° and added with suitable weights to minimize the foreground power in the combined map. The details of the ILC procedure are given in (Bennett et al., 2003c). In Fig. [12] we compare the power extracted by our implementation of the ILC procedure with that obtained by WMAP. We find that the two are in good agreement with one another.

In earlier papers, it has been shown that both the IPSE and ILC procedures are expected to have some bias at low l . The foreground cleaning procedure removes some extra power and hence the extracted signal is lower in comparison to the real signal. This effect is dominant at low multipoles $l = 2, 3$. Here we compute this bias for ILC using 600 simulations. The extracted bias is also shown in Fig. [12]. As expected we find a negative bias at low- l in power spectrum estimation (Hinshaw et al., 2007; Saha et al., 2008; Chiang, Naselsky & Coles, 2009). However we find that the bias is much smaller in comparison to that obtained using IPSE. The final power spectrum after removing this negative bias is also shown in Fig. [12].

In Fig. [13] we have shown both the statistics computed for the ILC cleaned map. The corresponding statistical significance using the two statistics is shown in Fig. [14]. The results were presented for the WMAP seven year ILC map, the ILC map obtained by us as well as the low- l bias corrected ILC power. We find that the statistical significance of all the three maps are comparable to one another. We note that the ILC map is reliable on angular scales greater than 10° (Bennett et al., 2003c). It is available at a resolution of 1° and so is HILC map of (Kim, Naselsky & Christensen, 2008). So, it will not be meaningful to assess the parity preference in that data at high l , even if it shows such an asymmetry, where its power spectrum deviates away from the theoretical CMB power spectrum.

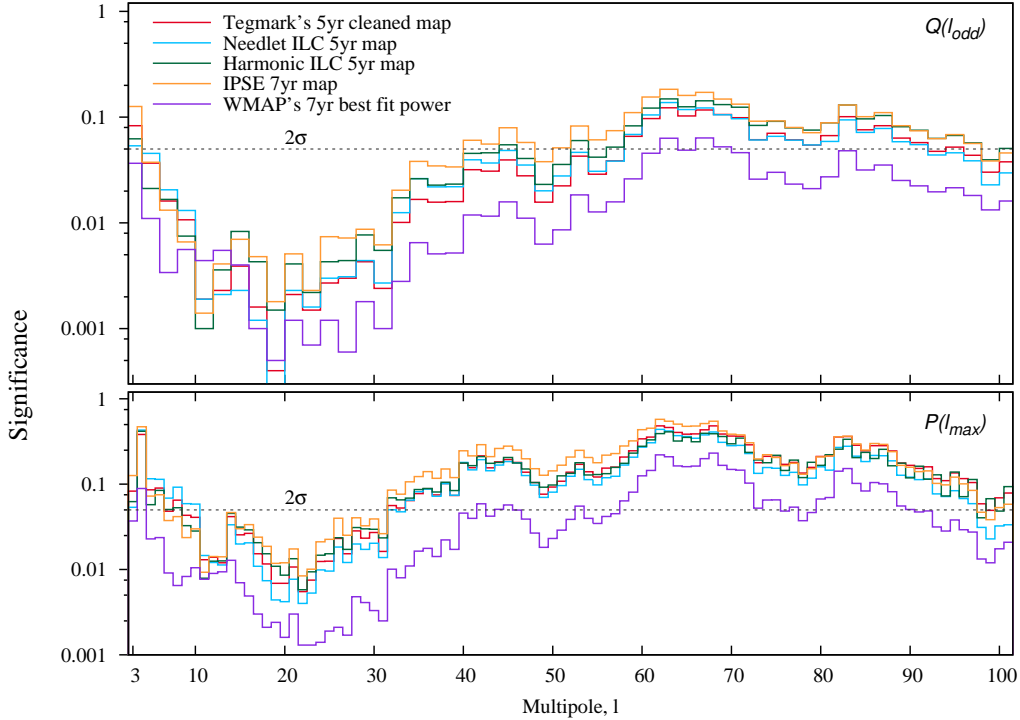


Figure 10: The significance using the pseudo- C_l estimator. The different maps mentioned in the legend are masked using $KQ85yr7$ mask.

6 Parity significance with low- l cuts

From Fig. [1], we see that the values of both the statistics, $Q(l)$ and $P(l_{max})$, are much lower at small ' l '. This is also reflected in Fig. [2] and Fig. [3] where the p -values are found to be relatively insignificant at low- l . Also, as mentioned earlier, many studies found that the low- l are associated with various anomalies. Hence it is reasonable to assess the parity asymmetry neglecting some of the low- l multipoles. In order to get a better insight into this parity asymmetry issue and avoid any “anomalous low- l ” concerns, we discard some low- l values in this analysis and compute both the statistics for WMAP data and assess its significance. Thus our statistic now becomes,

$$Q(l_{odd}) = \frac{2}{l_{odd} - l_{cut} + 1} \sum_{l=l_{cut}}^{l_{odd}} \frac{\mathbb{C}_{l-1}}{\mathbb{C}_l}, \quad (11)$$

where l_{cut} is any odd $l > 3$ and the summation is again over all odd multipoles $\leq l_{odd}$. We implement a similar l -cut for $P(l_{max})$ at low- l in computing P^+ and P^- .

The result of applying the two statistics to WMAP best fit power with various low- l cuts is shown in Fig. [15]. As can be seen, both the asymmetry statistics rises closer to one with increasing multipole cuts. With different low- l cuts, the p -values at various l in the range $l = [l_{cut}, 101]$ are computed for both the statistics and the results are given in Fig. [16] and in Fig. [17]. We see from these figures that the significance of parity asymmetry immediately starts decreasing and falls below 2σ just by ignoring the first 6 multipoles ($l = 2, \dots, 7$). This happens with both the statistics. It shows that the dominant contribution to the parity asymmetry arises from a few low l multipoles only. It raises the interesting possibility that this might be related to the other low- l anomalies seen in the WMAP data. These might arise from a common physical origin.

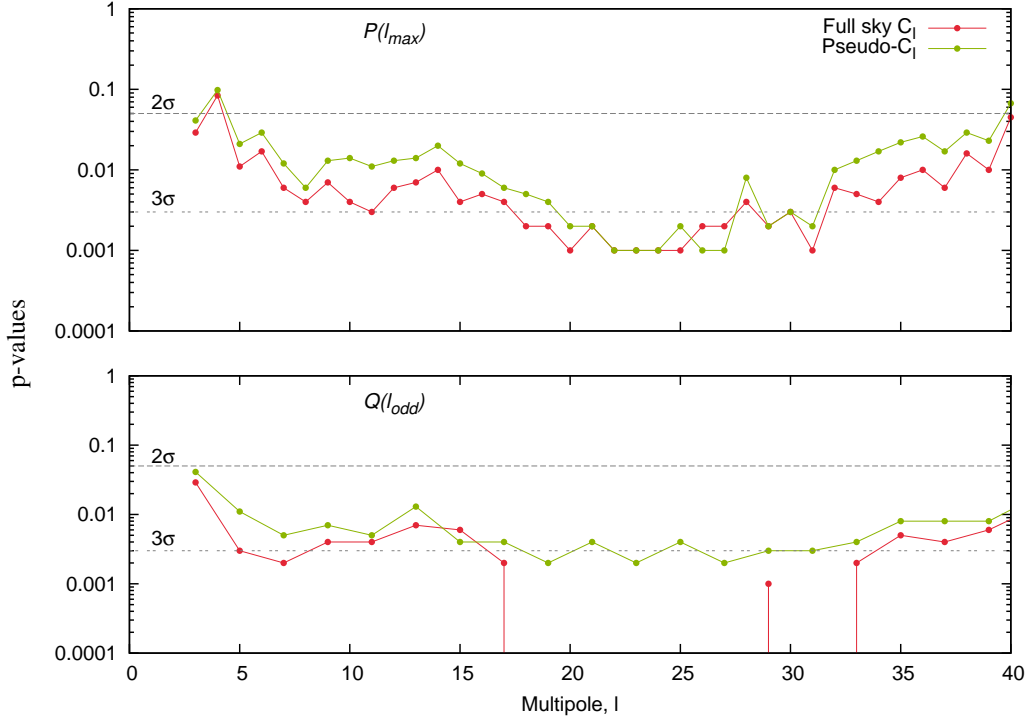


Figure 11: The significance for the WMAP best fit power spectrum using masked sky random realizations of pure CMB. The results where the power spectrum of random realizations is estimated from full sky maps is shown for comparison.

7 Conclusions

We have analysed the signature of parity asymmetry, recently found in WMAP’s best fit temperature power spectrum, in considerable detail in the multipole range $l = [2, 101]$. For this purpose, we used the statistic, $P(l_{max})$, introduced earlier as well as a new measure, $Q(l_{odd})$, which appears to be more sensitive. We confirm the signal of parity asymmetry at significance level of 3σ . By comparing an ensemble of simulated foreground cleaned maps with the WMAP best fit power spectrum, we deduce that the observed parity asymmetry cannot be attributed to foreground cleaning or residual foregrounds. Here we use the foreground templates from PSM. The PSM may not correctly model some sub-dominant or unknown foregrounds. Hence we created some templates which explicitly violate parity and included them in our analysis as both additive and multiplicative modulation to CMB. We again find that these cannot explain the observed power asymmetry. The level of asymmetry present in data can be obtained by introducing an unrealistically large value of these foreground components. Hence we find that we are unable to attribute the observed signal to foreground cleaning or residual foregrounds.

We next tested the presence of this signal of parity asymmetry in several other foreground cleaned maps such as the IPSE map, cleaned map using the procedure of Tegmark, de Oliveira-Costa & Hamilton, 2003, Needlet ILC map and Harmonic ILC map. We find that these maps also show a signal of parity asymmetry provided we use the pseudo- C_l estimator after applying a mask in order to eliminate the heavily foreground contaminated regions. The significance level for these maps, however, is found to be not as high as that in the case of WMAP best fit power. The ILC map also shows parity asymmetry with results closer to that obtained with the WMAP best fit power spectrum.

Finally, we tested the WMAP data for parity asymmetry by eliminating some of the low- l modes. The low- l multipoles are known to show some anomalous results such as low quadrupole power (Bennett et al. 2003b), alignment of various multipoles (de Oliveira-Costa et al., 2004) etc. Hence it is possible that

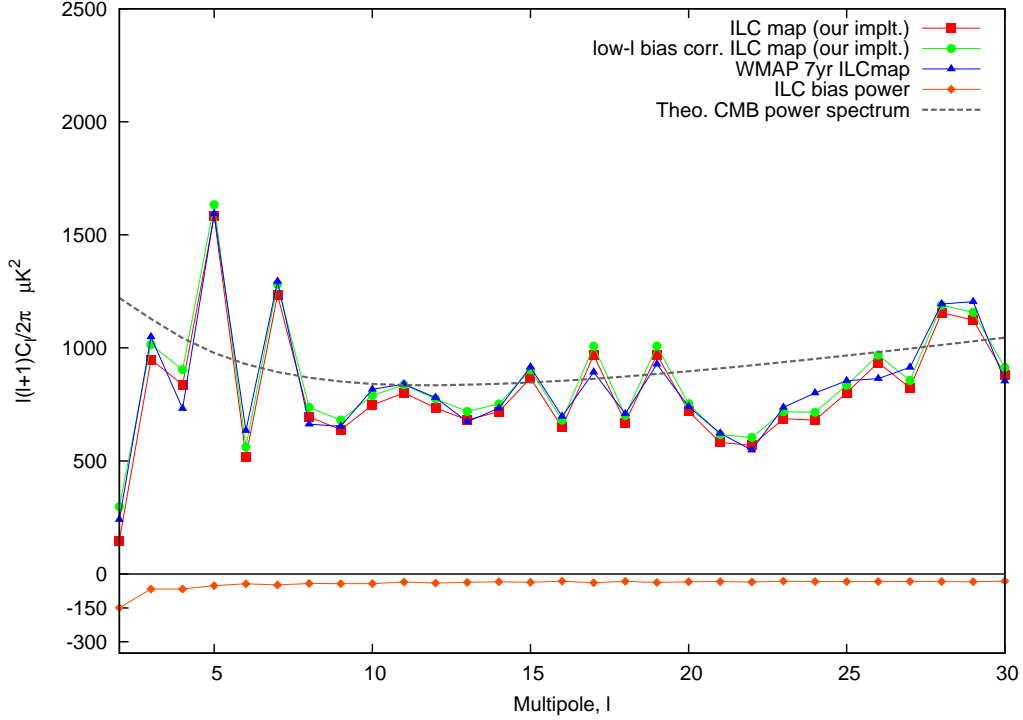


Figure 12: Power spectrum of ILC cleaned map from our implementation and from the WMAP seven year ILC map is plotted here. The curve below zero of y-axis is the bias in the power spectrum from ILC cleaning method. This is computed as an average over 600 simulated pure maps and clean maps generated at 1° resolution. Also shown is the best fit theoretical CMB temperature power spectrum for comparison. Our implementation and WMAP cleaned ILC map agree with each other. Any difference could be due to our bias correction map estimated using PSM. WMAP uses MEM foreground templates for generating the foreground bias map.

the parity asymmetry might also get a large contribution from these multipoles. We found that the parity asymmetry disappears by just ignoring the first six multipoles ($l = 2, \dots, 7$). Hence we conclude that the low- l multipoles give dominant contribution to the signal of parity asymmetry. It is, therefore, possible that all the low- l anomalies, including the parity asymmetry might have a common origin.

Acknowledgements

We acknowledge the use of WMAP data available from NASA's LAMBDA site (<http://lambda.gsfc.nasa.gov/>). We also used the publicly available HEALPix software (Gorski et al., 2005) for map handling and also to extract relevant information from these maps. We thank John P. Ralston for useful discussions. We thank Pavel Naselsky for a useful communication.

References

- A. Ben-David, E. D. Kovetz, N. Itzhaki, 2011, arXiv:1108.1702
- C. L. Bennett et al., 2003a, ApJ, 583, 1
- C. L. Bennett et al., 2003b, ApJS, 148, 1
- C. L. Bennett et al., 2003c, ApJS, 148, 97
- C. L. Bennett et al., 2011, ApJS, 192, 17

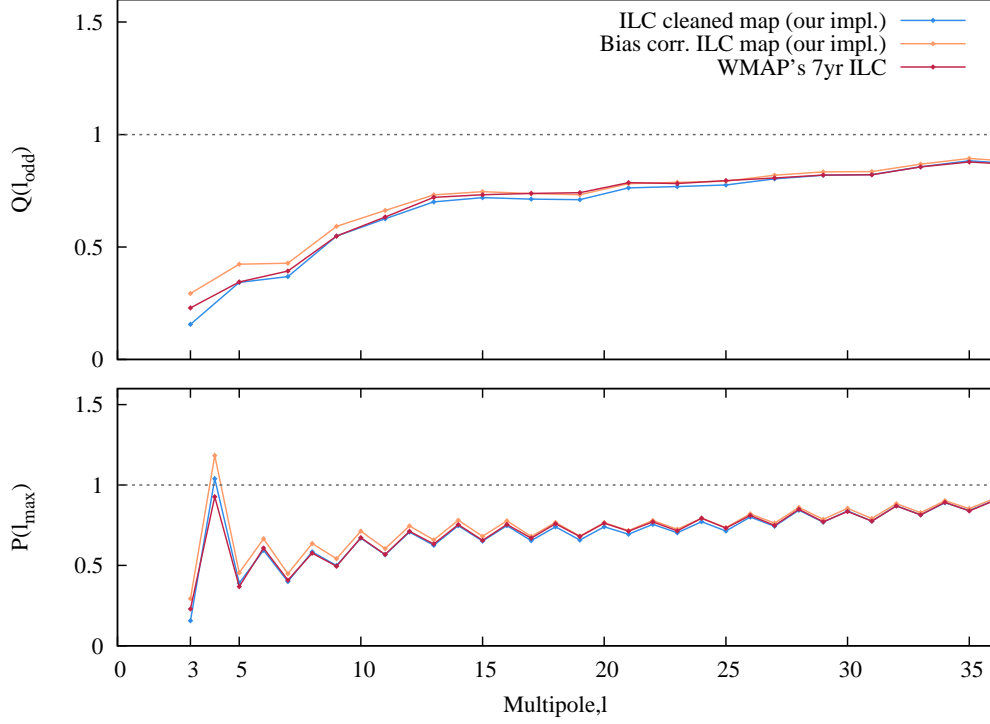


Figure 13: The two statistics applied to ILC cleaned WMAP seven year data. The statistics are shown for the ILC cleaned map as cleaned by us, bias corrected ILC power and WMAP's ILC 7yr map.

- A. Bernui, B. Mota, M. J. Reboucas and R. Tavakol, 2007, *Int. J. of Mod. Phys. D*, 16, 411
- P. Bielewicz, H. K. Eriksen, A. J. Banday, K. M. Gorski and P. B. Lilje, 2005, *ApJ*, 635, 750
- F. R. Bouchet and R. Gispert, 1999, *New Astron.*, 4, 443
- E. F. Bunn and A. Bourdon, 2008, *Phys. Rev. D*, 78, 123509
- L-Y. Chiang, P. D. Naselsky and P. Coles, 2009, *ApJ*, 694, 339
- C. J. Copi, D. Huterer and G. D. Starkman, 2004, *Phys. Rev. D*, 70, 043515
- C. J. Copi, D. Huterer, D. J. Schwarz and G. D. Starkman, 2007, *Phys. Rev. D*, 75, 023507
- C. J. Copi, D. Huterer, D. J. Schwarz and G. D. Starkman, 2010, *Advances in Astronomy*, 847541
- C. J. Copi, D. Huterer, D. J. Schwarz and G. D. Starkman, 2011, *arXiv:1103.3505*
- A. de Oliveira-Costa et al., 2002, *ApJ*, 567, 363
- A. de Oliveira-Costa, M. Tegmark, M. Zaldarriaga and A. Hamilton, 2004, *Phys. Rev. D*, 69, 063516
- A. de Oliveira-Costa and M. Tegmark, 2006, *Phys. Rev. D*, 74, 023005
- J. Delabrouille et al., 2009, *A&A*, 493, 835
- G. Dobler and D. P. Finkbeiner, 2008a, *ApJ*, 680, 1222
- G. Dobler and D. P. Finkbeiner, 2008b, *ApJ*, 680, 1235
- G. Efstathiou, 2003, *MNRAS*, 346, 2, L26

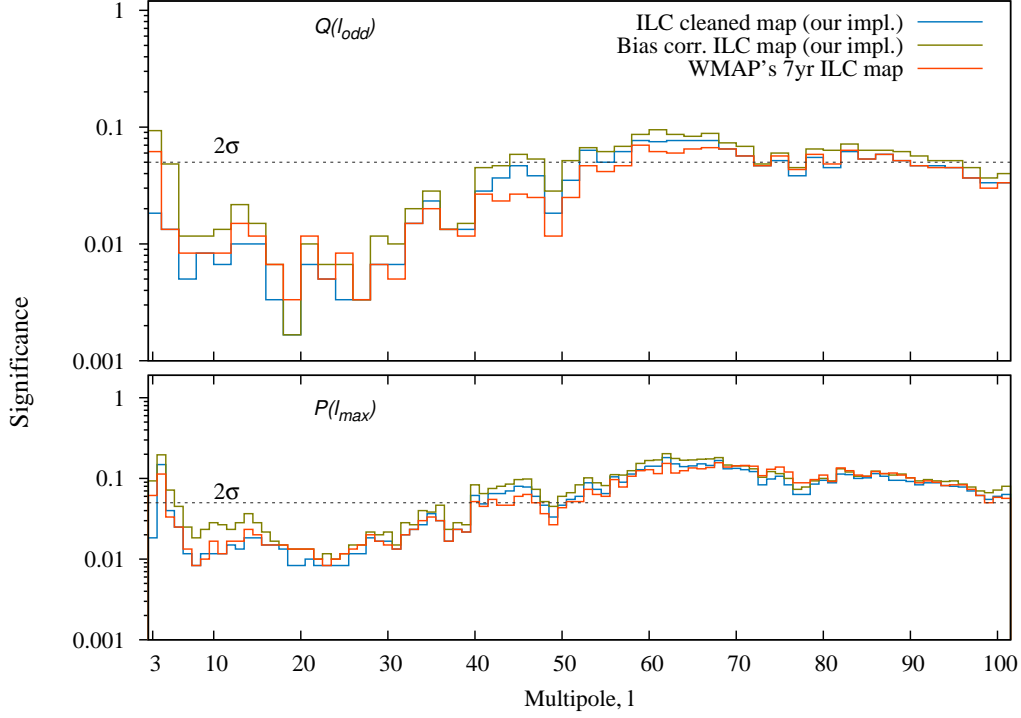


Figure 14: The p -values of the power asymmetry from the ILC cleaned data. Shown here are the probability estimates for the two statistics from ILC map as cleaned by us, bias corrected ILC map from our implementation and the WMAP team cleaned seven year ILC map. As seen, the probability of the parity asymmetry is lower compared to the WMAP's seven year best fit power. However the probability rises slightly after correcting for the low- l bias.

G. Efstathiou, Y-Z. Ma and D. Hanson, 2010, MNRAS, 407, 2530

H. K. Eriksen, F. K. Hansen, A. J. Banday, K. M. Gorski and P. B. Lilje, 2004a, ApJ, 605, 14

H. K. Eriksen, D. I. Novikov, P. B. Lilje, A. J. Banday and K. M. Gorski, 2004b, ApJ, 612, 64

H. K. Eriksen, A. J. Banday, K. M. Gorski and P. B. Lilje, 2004c, ApJ, 612, 633

H. K. Eriksen et al., 2007a, ApJ, 656, 641

H. K. Eriksen, A. J. Banday, K. M. Gorski, F. K. Hansen and P. B. Lilje, 2007b, ApJ, 660, 2, L81

C. Gordon, W. Hu, D. Huterer and T. Crawford, 2005, Phys. Rev. D, 72, 103002

K. M. Gorski et al., 2005, ApJ, 622, 759

N. E. Groeneboom, M. Axelsson, D. F. Mota and T. Koivisto, arXiv:1011.5353

A. Gruppuso et al., 2011, MNRAS, 411, 1445

V. G. Gurzadyan, A. A. Starobinsky, A. L. Kashin, H. G. Khachatryan and G. Yegorian, 2007, Mod. Phys. Lett. A, 22, 39, 2955

M. Hansen, A. M. Frejsel, J. Kim, P. Naselsky and F. Nesti, 2011, Phys. Rev. D, 83, 103508

D. Hanson and A. Lewis, 2009, Phys. Rev. D, 80, 063004

G. Hinshaw et al., 2003, ApJS, 148, 135

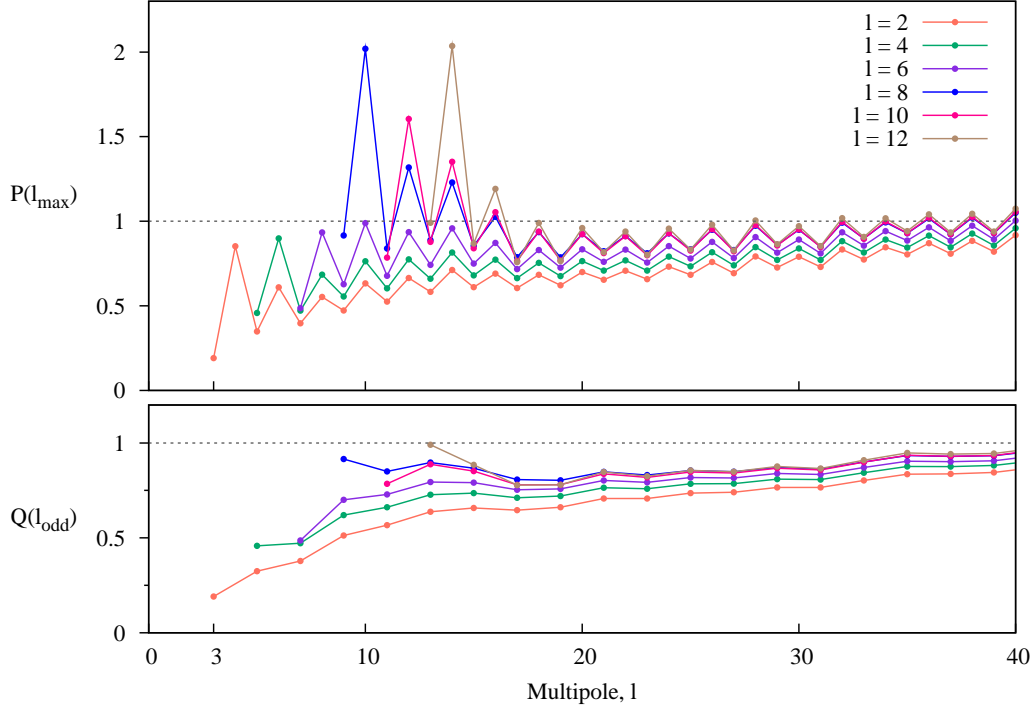


Figure 15: The parity preference estimators $Q(l)$ and $P(l_{max})$ with various low- l cuts as applied to WMAP seven year best fit power spectrum. We see that the estimators steadily rise close to one with increasing low- l cut.

G. Hinshaw et al., 2007, ApJS, 170, 288

E. Hivon et al., 2002, ApJ, 567, 2

K. Ichiki, R. Nagata, J. Yokoyama, 2010, Phys. Rev. D, 81, 083010

N. Jarosik et al., 2011, ApJS, 192, 14

J. Kim, P. Naselsky and P. R. Christensen, 2008, Phys. Rev. D, 77, 103002

J. Kim and P. Naselsky, 2010, ApJ, 714, L265

A. Kogut et al., 1996, ApJ, 464, L5

A. Kogut et al., 2003, ApJS, 148, 161

E. Komatsu et al., 2011, ApJS, 192, 18

T. S. Koivisto and D. F. Mota, 2011, JHEP, 02, 061

K. Land and J. Magueijo, 2005a, Phys. Rev. Lett., 95, 071301

K. Land and J. Magueijo, 2005b, Phys. Rev. D, 72, 101302

D. Larson et al., 2011, ApJS, 192, 16

M. Maris, C. Burigana, A. Gruppuso, F. Finelli and J. M. Diego, 2011, MNRAS, 415, 2546

J. Martin, C. Ringeval, 2004, Phys. Rev. D, 69, 083515

J. Martin, C. Ringeval, 2006, JCAP, 08, 009

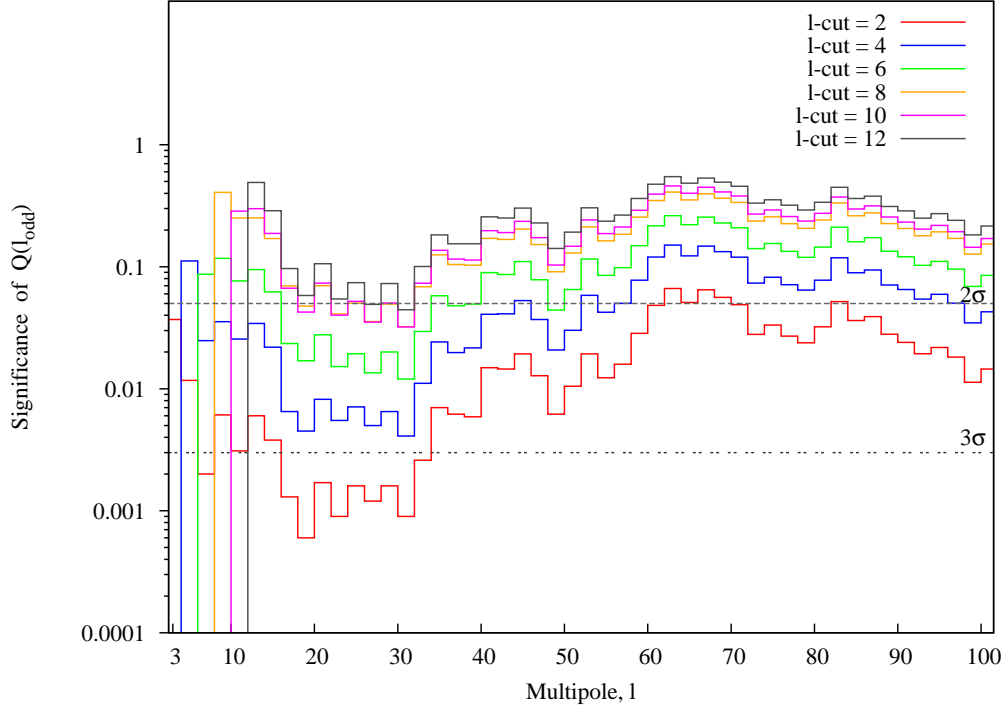


Figure 16: The p - values of our parity preference estimator, $Q(l)$, as applied to WMAP’s best fit power with various low- l cuts, using an ensemble of 10,000 pure CMB realizations. The significance falls below 95% CL just by ignoring the first 6 multipoles.

L. Page et al., 2003, ApJS, 148, 233

Planck “Blue Book”, Planck Collaboration 2005, Planck : The Scientific Programme, ESA Publication, ESA-SCI(2005)01

A. Pontzen and H. V. Peiris, 2010, Phys. Rev. D, 81, 103008

J. P. Ralston and P. Jain, 2004, Int. J. Mod. Phys. D, 13, 1857

R. Saha, P. Jain and T. Souradeep, 2006, ApJ, 645, L89

R. Saha, S. Prunet, P. Jain and T. Souradeep, 2008, Phys. Rev. D, 78, 023003

P. K. Samal, R. Saha, P. Jain and J. P. Ralston, 2008, MNRAS, 385, 1718

P. K. Samal et al., 2010, ApJ, 714, 840

D. J. Schwarz, G. D. Starkman, D. Huterer and C. J. Copi, 2004, Phys. Rev. Lett., 93, 221301

D. N. Spergel et al., 2003, ApJS, 148, 175

M. Tegmark, A. de Oliveira-Costa and A. J. S. Hamilton, 2003, Phys. Rev. D, 68, 123523

M. S. Turner, 1983, Phys. Rev. D, 28, 1243

X. Wang, B. Feng, M. Li, X-L. Chen, X. Zhang, 2005, Int. J. Mod. Phys. D, 14, 1347

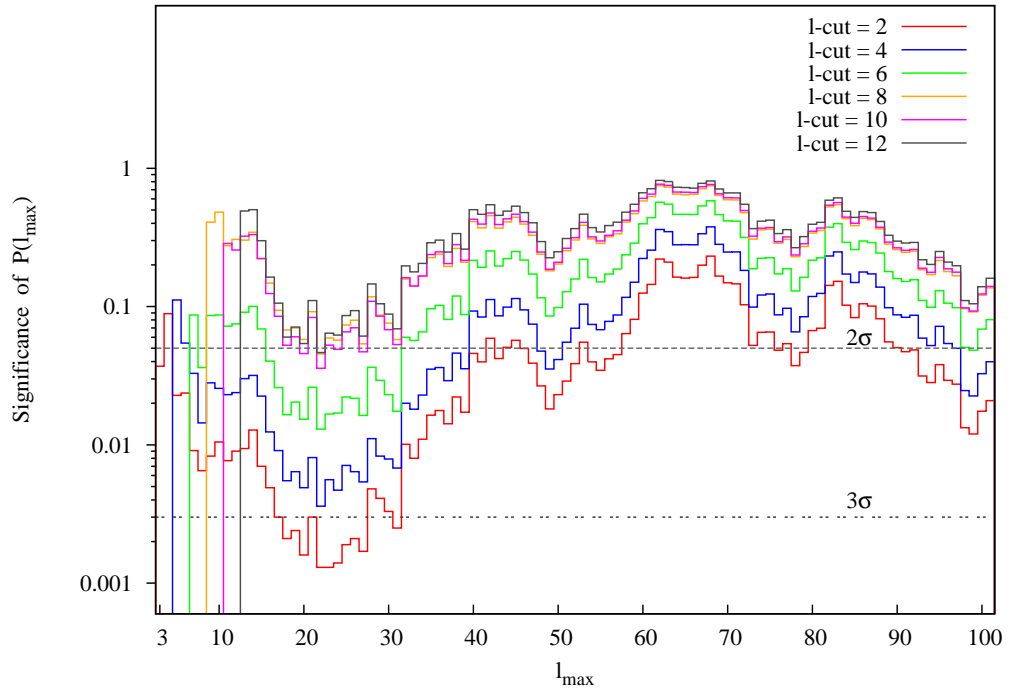


Figure 17: Same as Fig. [16] but for $P(l)$ statistic. Here too we find that the significance we found earlier disappears by ignoring the first 6 multipoles.